Flexible micro-supercapacitors with high energy density from simple transfer of photoresist-derived porous carbon electrodes

Mun Sek Kim, Ben Hsia, Carlo Carraro, Roya Maboudian [*]

Department of Chemical and Biomolecular Engineering, University of California at Berkeley, Berkeley, CA 94720, USA

ARTICLE INFO

ABSTRACT

Flexible integrated micro-scale energy storage has attracted increasing research interest due to numerous compelling device applications. This paper presents a facile and scalable technique to fabricate a flexible high surface area carbon based micro-supercapacitor via pyrolysis of a commercial photoresist and transfer to a flexible substrate. Cyclic voltammetry, galvanostatic charge/discharge, and AC impedance spectroscopy are used to characterize the fabricated devices, which show near ideal electrochemical behavior and retention of initial electrochemical performance after 300 bending cycles. The devices exhibit maximum energy density of $1\,mWh\,cm^{-3}$ in aqueous electrolyte, which compares favorably to state-of-the-art flexible and rigid carbon-based micro-supercapacitor devices.

© 2014 Elsevier Ltd. All rights reserved.

1. Introduction

Supercapacitors are electrochemical energy storage devices that typically have high power density, long cycle lifetime, low environmental impact, and safe operation relative to current battery technologies [1–6]. Micro-scale supercapacitors, or "micro-supercapacitors," can be integrated with the micro-devices they power, simplifying fabrication and maintaining small form factors. In particular, micro-supercapacitors can enable technologies that require fast cycling and/or infrequent maintenance such as wireless sensor networks, implantable biomedical devices, and autonomous microrobots [2,7,8]. Most commonly, micro-supercapacitors are fabricated on rigid substrates such as Si, but growing interest in flexible electronics applications such as wearable electronics and roll-up displays has stimulated the development of flexible energy storage solutions, including flexible micro-supercapacitors [8–10].

A common electrode material used in conventional supercapacitors is activated carbon [2,3,11], which has a high surface area to volume ratio and is earth abundant and inexpensive. For micro-supercapacitors, however, activated carbon is difficult to deposit and pattern on the micro-scale [12], and hence, other carbon-based electrodes have been investigated, such as onion-like carbon [5], inkjet printed activated carbon [13], carbon nanotubes [14], carbide-derived carbons [12,15,16], graphene [17–20], reduced graphene oxide and carbon nanotube composites [21], graphene/carbon nanotube carpets [22], and photoresist-derived carbon [23]. However, limited work has been reported on the development of carbon-based flexible micro-supercapacitors. Possible candidates for micro-supercapacitor electrode materials that can be deposited directly on flexible substrates include pseudocapacitive polymers such as polypyrrole [8] and polyaniline [24], and carbon-based electrodes including laser-scribed graphene oxide [17], reduced graphene oxide [18], and inkjet-printed graphene [19].

Another promising method for flexible micro-supercapacitor fabrication is the transfer of prepatterned electrodes onto flexible substrates, analogous to the dry transfer of carbon nanotubes onto polymer substrates for flexible electronics [25,26]. This technique has the advantage of good device-to-substrate adhesion [25] and allows for the use of high temperature-processed materials on polymer substrates, which would otherwise be impossible given the limitations imposed by glass transition temperature of many polymers. Additionally, lithographic patterning can be done using traditional microfabrication processes designed for rigid substrates prior to transfer. In this study, pyrolysis of patterned photoresist is used to form high specific surface area carbon electrodes [23]. This technique is simple and can utilize existing microfabrication infrastructure for easy integration with micro-devices. The subsequent transfer to a polymer substrate is demonstrated to yield a robust, flexible micro-supercapacitor device with good electrochemical performance.

2.   Experimental

2.1.   Sample preparation

Fig. 1a shows a schematic illustration of the flexible planar microsupercapacitor fabrication process. The synthesis of the photoresist-derived carbon film is previously described in detail [23]. Briefly, a layer of SiO_2 is deposited via thermal oxidation on a 4″ Si(100) wafer. Then, a commercial positive photoresist, (PR, SPR-220-7.0) is spin-coated onto the wafer without any pretreatment and is patterned in a two-pad configuration using photolithography. The sample is loaded into a horizontal hot-wall tube furnace (Thermo Scientific Lindberg Blue M) and prebaked at 300 °C in 1 Torr Ar (Praxair) for

30 min to drive off water and volatile solvents. Then, the temperature is increased to 900 °C in the same ambient at an approximate rate of 40 °C/min. Once 900 °C is reached, the gas is changed to 10% H_2/90% Ar (Praxair) and the sample is held at 900 °C for 1 h. The sample is then cooled at a rate of about 25 °C/min to room temperature in the same H_2/Ar gas environment. The size and shape of the pyrolyzed electrodes are identical to that of the patterned photoresist, demonstrating the good pattern fidelity post-pyrolysis (Fig. 1b). For the results presented in this paper, the electrodes have 3.7 mm width, 8.4 mm length, and 0.9 μm thickness, with an inter-electrode gap distance of 1.1 mm. After pyrolysis, a double-transfer process is used to move the patterned electrodes to a flexible substrate. First, the pyrolyzed-PR film is transferred to polycarbonate (PC, thickness of 100 μm, McMaster-Carr) by melting the PC onto the sample at 300 °C in air for 3 min. After cooling to room temperature, the PC is carefully peeled off from the substrate. The carbon preferentially adheres to the PC, and the electrodes are cleanly removed from the substrate. Then, a polyethylene film (PE, thickness of 100 μm, McMaster-Carr) is applied to the exposed surface of the transferred carbon film by melting the PE to the polycarbonate at 200 °C in air for 5 min. During this process, a pressure of about 18 kPa is applied on the top of the sample to reduce curling from any thermal mismatch and to maximize the adhesion between the carbon and the polyethylene films. After cooling to room temperature, the transferred film with PC and PE is immersed in methylene chloride solution overnight to dissolve the PC. Fig. 1c shows an optical image of the device after the 2nd transfer. As will be discussed, a double transfer process is necessary, as the surface of the carbon film after one transfer is found to have significantly different morphological and electrochemical properties than the opposite surface.
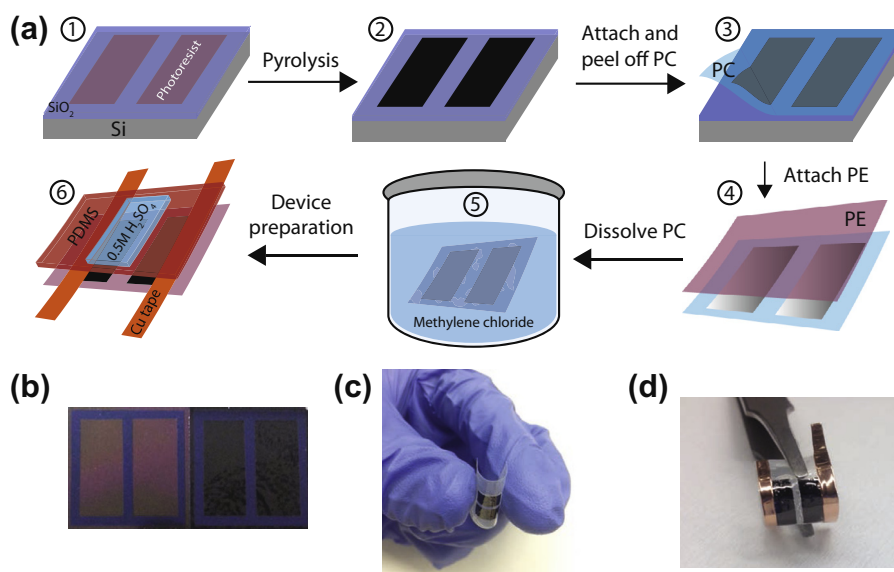

Fig. 1 – (a) Schematic illustration of flexible micro-supercapacitor fabrication process. PC is polycarbonate, PE is polyethylene, PDMS is polydimethylsiloxane. Photographs of (b) patterned photoresist electrodes before (left) and after (right) pyrolysis, (c) photoresist-derived carbon electrodes transferred to polyethylene and being flexed and (d) fully-fabricated device. (A color version of this figure can be viewed online.)

2.2. Characterization methods

The surface roughness of the carbon film is investigated via atomic force microscopy (AFM, Digital Instruments Nanoscope IIIa) in tapping mode. The surface wettability is probed via water contact angle measurements (Rame Hart Model 290).

The electrochemical performance of the flexible microsupercapacitor is measured via cyclic voltammetry (CV), galvanostatic charge/discharge, and AC impedance spectroscopy using a commercial potentiostat (AC Instruments, 660D Model). To obtain these measurements, an adhesive conductive tape (Cu/Ni tape, Ted Pella, #16067) is connected to the edge of each carbon film pad (see Fig. 1d), and a polydimethylsiloxane (PDMS) stamp is used to isolate the conductive tape from the electrolyte (step 6 in Fig. 1a). A central hole is cut into the PDMS and filled with electrolyte for testing. All the electrochemical measurements are performed in an aqueous electrolyte of 0.5 M H_2SO_4.

3. Results and discussion

3.1. Comparison of single and double-transferred electrodes

Due to the temperature limitations of most bulk flexible materials, many substrates would not survive the pyrolysis temperatures required to form conductive high surface area carbon films. Therefore, in order to fabricate a flexible device using pyrolyzed photoresist electrodes, post-pyrolysis transfer to a flexible substrate is required. However, a single transfer is found to yield a different film surface relative to the as-pyrolyzed surface. The first transfer (step 3 in Fig. 1a) exposes the electrode surface which is at the photoresist/substrate interface during pyrolysis, and hence, this surface is denoted as the "bottom" film surface, while the second transfer (step 5 in Fig. 1a) re-exposes the surface in contact with the gas (H_2 and Ar) during pyrolysis, and is denoted as the "top" surface. In this study, both the top and bottom surfaces are examined to compare the differences in electrochemical performance.

The AFM images of the top (as measured before transfer) and bottom (as measured after first transfer) of the carbon film, shown in Fig. 2, illustrate the morphological differences in the two surfaces. The top surface of the film is significantly

rougher than the bottom with RMS roughness of 1.3 and <0.3 nm, respectively. The bottom surface also shows no apparent porosity. This difference results from two experimental factors: first, the bottom surface of the photoresist is in contact with the smooth oxide substrate during pyrolysis, leading it to form a matching smooth surface; and second, the mechanism of pore formation during pyrolysis involves the vaporization of volatile photoresist components (which escape from the vapor/photoresist interface), and the etching effects of H_2 (which is present only at the vapor/photoresist interface) [23,27]. Transport limitations may not allow these processes to propagate all the way through the film thickness.

In accordance with the AFM results, CV results show that the top surface, obtained by double transfer, yields about 75 times higher areal capacitance at a scan rate of 100 mV s^{-1} compared to the bottom surface, obtained after single transfer (Fig. 3). The bottom of the film yields an areal capacitance of ~10 µF cm^{-2}, a value that is about two times higher than that of a smooth film [28]. The specific areal capacitance of the top surface is measured to be significantly higher, 0.75 mF cm^{-2}, in agreement with our previous work with untransferred, unpatterned photoresist-derived carbon films [23]. Water contact angle measurements are performed to compare the wetting of both surfaces. The top and bottom surfaces yield contact angles of 12° and 60° respectively, which confirms that the top surface is more hydrophilic than the bottom surface, resulting in more effective wetting of the pores by aqueous electrolytes. A double-transfer process is therefore necessary to obtain high energy density for the device.

3.2. Electrochemical performance

The CV curves of the flexible micro-supercapacitor at several different scan rates are shown in Fig. 4. The CV shape is semi-rectangular at scan rates of up to 10 V s^{-1}, indicating ideal capacitive performance (see Fig. 4a–c). Since the CV curves retain a rectangular form even at the high scan rate of 10 V s^{-1}, this is a good indication of the high-power capability of the device. The skewing of the CV shape at higher scan rates indicates some power limitations arising from the electrode resistance as well as the electrolyte resistance in the pores [29]. Our previous work suggests that the carbon film consists of a highly porous network [23], leading to possible mass trans-
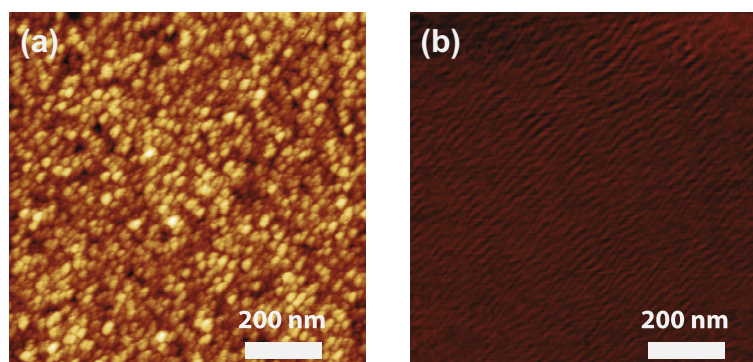

Fig. 2 – AFM images of the (a) top and (b) bottom surface of the pyrolyzed photoresist-derived carbon film. Both images have a z-scale of 10 nm. (A color version of this figure can be viewed online.)
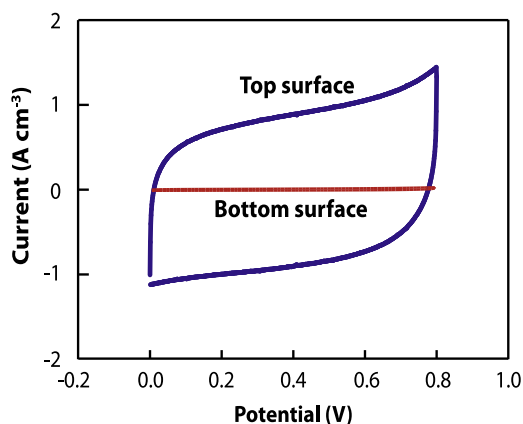
Fig. 3 – Cyclic voltammograms obtained on the photoresist-derived carbon electrode after one transfer (bottom surface) and after two transfers (top surface). The scan rate used is 100 mV s⁻¹. Electrolyte used is 0.5 M H₂SO₄. (A color version of this figure can be viewed online.)

fer limitations. Therefore, at higher scan rates, where the ions must access the micro-pores inside of the film in a short amount of time, the capacitance of the film is lower [30]. Fig. 4d, which shows higher capacitance at lower scan rates, illustrates this effect. The volumetric capacitance of the device is calculated from Eq. (1):

$$C = \frac{I}{\Delta V/\Delta t} \cdot \frac{1}{A \cdot t_f} \tag{1}$$

where C is the volumetric capacitance in F cm⁻³, I is the average current magnitude over the positive and negative sweep at a specific scan rate, $\Delta V/\Delta t$ is the scan rate, A is the projected active area of both electrodes, and t_f is the thickness of the carbon film (measured via cross-sectional SEM, 0.9 μm) [23]. The active area includes only the portion of electrode directly in contact with electrolyte. Volumetric data, rather than gravimetric data, are presented, as mass-based measurements are less meaningful for micro-scale applications [31,32]. The calculated volumetric capacitance of the device ranges from 1.7 to 11 F cm⁻³ over the tested scan rates. Lifetime CV cycling shows that the flexible micro-supercapacitor exhibits robust cycling stability, maintaining ~86% of the initial capacitance over 10,000 complete charge/discharge cycles as shown in Fig. 4e.

Galvanostatic charge/discharge has been performed at various currents densities, up to nearly 0.5 kA cm⁻³. The charge/discharge curves are linear, indicating ideal capacitive behavior (see Fig. 5a and b). A small IR drop can be seen at the start of each discharge cycle, with larger drops seen at higher current densities. The volumetric capacitance can be calculated from Eq. (1), as done for the CV, where I is now the applied current, ΔV is the voltage window excluding the IR drop during discharging, and Δt is the time required to discharge to 0 V. The equivalent series resistance values are approximated from Eq. (2):
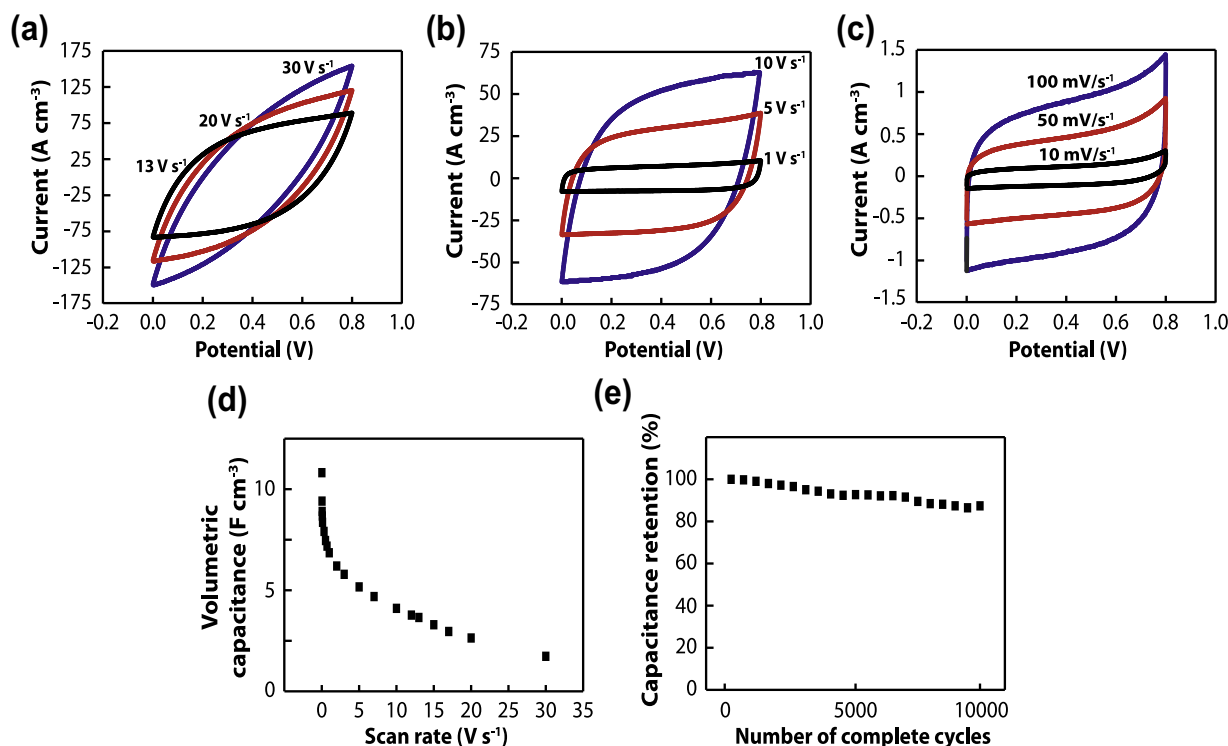
$$ESR = \frac{V_{drop}}{2 \cdot I} A \tag{2}$$

Fig. 4 – Cyclic voltammograms of fabricated flexible micro-supercapacitor at scan rates of (a) 13–30 V s⁻¹, (b) 1–10 V s⁻¹, and (c) 10–100 mV s⁻¹. (d) Calculated volumetric capacitance as a function of scan rate. (e) Lifetime of the flexible supercapacitor over 10,000 CV cycles from 0 to 0.8 V at a scan rate of 100 mV s⁻¹. Electrolyte used is 0.5 M H₂SO₄. All values are based on the total working electrode volume. (A color version of this figure can be viewed online.)

Fig. 5 – Galvanostatic charge/discharge curves of flexible micro-supercapacitor for different currents, (a) 3.1–31 mA cm^{-3}, (b) 65–463 A cm^{-3}, and (c) corresponding volumetric capacitances. Electrolyte used is 0.5 M H$_2$SO$_4$. All values are based on the total working electrode volume. (A color version of this figure can be viewed online.)
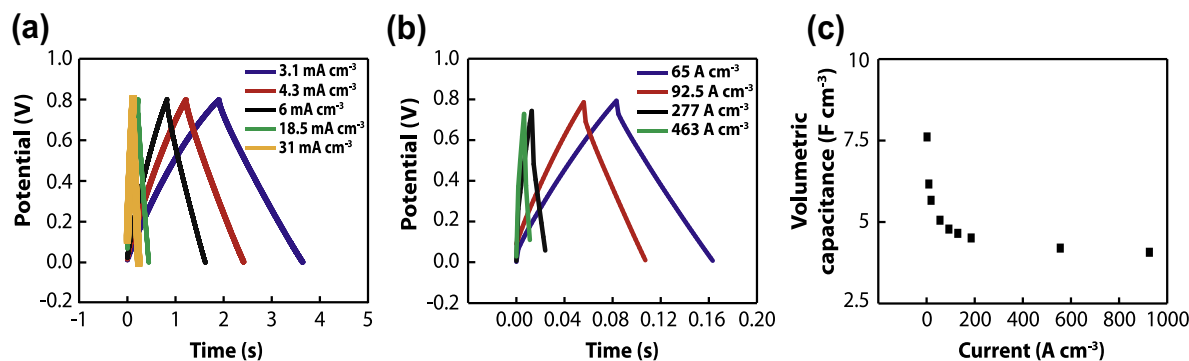
where V_{drop} is the magnitude of the IR drop, I is the applied discharge current, and A is the active area of both electrodes [33]. The capacitance values obtained via charge/discharge measurements show good agreement with the calculated capacitance from CV (see Fig. 5c). The ESR is calculated to be 8 Ω cm^2 at a current of 277 A cm^{-3}.

Another figure of merit for evaluating device cycling speed is the −45° phase angle crossover frequency, obtained from AC impedance data; a high frequency implies fast cycling performance. As seen in Fig. 6a, the −45° crossover frequency of our device is ∼122 Hz in the aqueous electrolyte. The crossover frequency value is somewhat lower than other high power microsupercapacitors fabricated on rigid substrates and measured in aqueous electrolytes, e.g., 200 Hz for reduced graphene oxide and carbon nanotube (rGO–CNT) composites [21], and 460–1343 Hz for graphene/carbon nanotube carpets-based micro-supercapacitors (G/CNTs–MCs) [22], but is significantly higher than other porous electrode materials such as activated carbon, which show −45° crossover frequencies of less than 10 Hz (estimated from impedance data in references [5] and [13]). Flexible micro-supercapacitors based on laser scribed graphene electrodes show a crossover

frequency of ∼50 Hz in aqueous solution, indicating that the device presented in this paper has a faster cycling performance [17]. The Nyquist plot shown in Fig. 6b shows a sub-vertical line which indicates a deviation from ideal capacitive behavior, likely due to the film's distribution of pore size leading to limited utilization of film micro-pores at high frequencies [34].

3.3. Energy and power density

The theoretical energy and power densities of the device are calculated from CV data using Eqs. (3) and (4):

$$E = \frac{1}{2}\frac{1}{3600} \cdot C \cdot \Delta V^2 \qquad (3)$$

$$P = \frac{3600 \cdot E}{\Delta t} \qquad (4)$$

where E is the energy density in Wh cm^{-3}, C is the volumetric capacitance in F cm^{-3}, ΔV is the operating voltage window in V, P is the power density in W cm^{-3}, and Δt is the discharge time in s. The flexible micro-supercapacitor presented in this paper provides outstanding energy density as shown in Fig. 7.
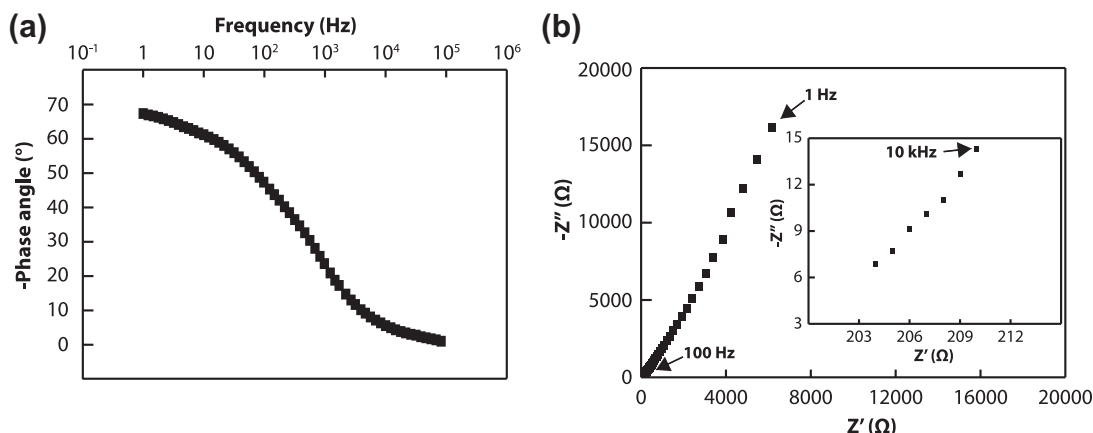

Fig. 6 – AC impedance spectroscopy results of flexible micro-supercapacitor with AC amplitude of 5 mV and DC voltage of 0 V. (a) Negative phase versus frequency plot for the micro-supercapacitor where the −45° crossover frequency is at 122 Hz. (b) Nyquist plot for the flexible micro-supercapacitor. The inset shows the high frequency regime. Electrolyte used is 0.5 M H$_2$SO$_4$.
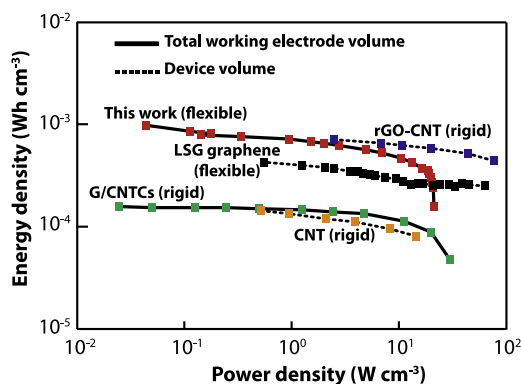
Fig. 7 – Ragone plot comparing the present flexible micro-supercapacitor to other micro-supercapacitors. All the results are measured in aqueous electrolytes. "Device volume" indicates that the energy and power density are given in reference to the volume of the fully-fabricated device including electrode, inter-electrode gap, and current collector volume. These density values will necessarily be smaller than the values given in reference to the electrode volume only. Laser-scribed graphene (LSG), reduced graphene oxide and carbon nanotube (rGO–CNT) & carbon nanotube (CNT), graphene and carbon nanotube carpet based micro-supercapacitor (G/CNTCs) data are obtained from Refs. [17,21,22] respectively. The type of substrate, flexible or rigid, is indicated in the plot. (A color version of this figure can be viewed online.)

The theoretical power and energy densities range from 0.05 to 56 W cm^{-3} and 0.8 to 1 Wh cm^{-3}, respectively. Despite a simple two-pad geometry and a rather simple fabrication process, the energy density is competitive with other recently reported flexible and rigid micro-supercapacitors measured in aqueous electrolytes [17,21,22]. The device does not yield the highest power density due to the transport limitations inherent in a porous network, but the achieved power is still competitive as indicated by the good CV performance at high scan rates and the high crossover frequency in the AC impedance results. Furthermore, a dense interdigitated electrode geometry has been shown to improve power performance in other carbon-based micro-supercapacitors and the simple geometry of the presented micro-supercapacitor likely further contributes to the power limitations due to the large mean ionic diffusion path [17]. Optimization of the electrode geometry for improved power performance is currently under investigation. Standard photolithography provides high resolution patterning of photoresist on the nanoscale; numerous geometries or configurations of electrodes can be fabricated and integrated on-chip with micro-devices.

3.4. Flexing performance

In order to determine the mechanical stability of the micro-supercapacitor upon flexing, the 1×1 cm^2 device is placed on the round surface of a cylinder with varied radii of 17.5, 12.5, and 5 mm. One end of the sample edge is fixed to the cylinder wall, and the other edge is manually bent to the cylinder surface and allowed to unbend. The device is bent 100 times
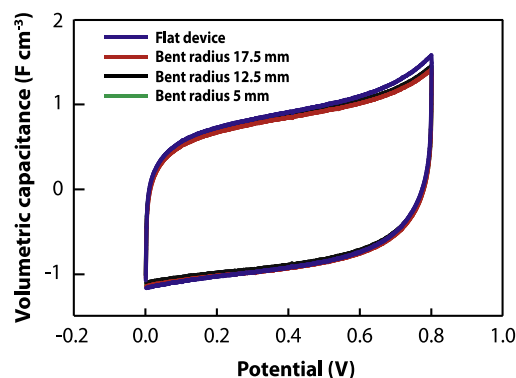

Fig. 8 – Cyclic voltammogram comparison of the device before and after 100 bending cycles at each indicated radius. Scan rate used is 100 mV s^{-1}. (A color version of this figure can be viewed online.)

at the largest radius of curvature, tested in the unbent configuration, bent 100 times at the next largest curvature, tested, and finally bent 100 times at the smallest curvature, resulting in 300 total bending cycles. Flexing tests show good capacitive performance retention after repeated bending. As seen in Fig. 8, the cyclic voltammogram shows a consistent rectangular shape at 100 mV s^{-1} after repetitive bending of the device at three different radii. There is only a ~2% deviation in the volumetric capacitance after 300 flexing cycles. Other flexible electrode materials such as laser-scribed graphene have been demonstrated to yield good micro-supercapacitor performance in the bent configuration, but robust mechanical stability has not yet been demonstrated [17], and is an important consideration for applications which require repeated flexing cycles. The flexible micro-supercapacitor presented in the work shows consistent performance after repeated flexing, demonstrating the mechanical stability of the film, and is therefore promising for flexible energy storage applications.

4. Conclusion

In summary, we have fabricated a flexible micro-supercapacitor using photoresist-derived carbon electrodes. The electrodes can be easily patterned and integrated for on-chip energy storage applications by using existing lithographic techniques. Furthermore, the electrode fabrication can be scaled to wafer-scale processing and the pyrolyzed electrodes can be easily transferred to flexible substrates while demonstrating excellent electrochemical performance including high energy and power densities, robust lifetime cycling performance, and high flexibility. This technique holds promise for the fabrication of high performance flexible micro-supercapacitors that are scalable and easily integrated with existing microfabrication technologies.

Acknowledgements

REFERENCES

[1] Conway BE. Electrochemical supercapacitors: scientific fundamentals and technological applications. New York: Kluwer Academic/Plenum Publishers; 1999.

[2] Simon P, Gogotsi Y. Materials for electrochemical capacitors. Nat Mater 2008;7:845–54.

[3] Frackowiak E, Beguin F. Carbon materials for the electrochemical storage of energy in capacitors. Carbon 2001;39:937–50.

[4] Zhang LL, Zhao XS. Carbon-based materials as supercapacitor electrodes. Chem Soc Rev 2009;38:2520–31.

[5] Pech D, Brunet M, Durou H, Huang P, Mochalin V, Gogotsi Y, et al. Ultrahigh-power micrometer-sized supercapacitors based on onion-like carbon. Nat Nanotechnol 2010;5:651–4.

[6] Beidaghi M, Wang C. Micro-supercapacitors based on interdigital electrodes of reduced graphene oxide and carbon nanotube composites with ultrahigh power handling performance. Adv Funct Mater 2012;22:4501–10.

[7] Simjee F, Chou PH. Everlast: long-life, supercapacitor-operated wireless sensor node. In: Proceedings, international symposium on low power electronics and design (ISLPED '06), Tegernsee (Germany), NY. New York: ACM/IEEE Press; 2006. p. 197–202..

[8] Sung JH, Kim SJ, Jeong SH, Kim EH, Lee KH. Flexible micro-supercapacitors. J Power Sources 2006;162:1467–70.

[9] Pushparaj VL, Shaijumon MM, Kumar A, Murugesan S, Ci L, Vajtai R, et al. Flexible energy storage devices based on nanocomposite paper. PNAS 2007;34:13574–7.

[10] Jain K, Klosner K, Zemel M, Raghunandan S. Flexible electronics and displays: high-resolution, roll-to-roll, projection lithography and photoablation processing technologies for high-throughput production. Proc IEEE 2005;8:1500–10.

[11] Gamby J, Taberna PL, Simon P, Fauvarque JF, Chesneau M. Studies and characterisations of various activated carbons used for carbon/carbon supercapacitors. J Power Sources 2001;101:109–16.

[12] Chmiola J, Largeot C, Tabema PL, Simon P, Gogotsi Y. Monolithic carbide-derived carbon films for micro-supercapacitors. Science 2010;328:480–3.

[13] Pech D, Brunet M, Taberna PL, Simon P, Fabre N, Mesnilgrente F, et al. Elaboration of a microstructured inkjet-printed carbon electrochemical capacitor. J Power Sources 2010;195:1266–9.

[14] Futaba DN, Hata K, Yamada T, Hiraoka T, Hayamizu Y, Kakudate Y, et al. Shape-engineerable and highly densely packed single-walled carbon nanotubes and their application as super-capacitor electrodes. Nat Mater 2006;5:987–94.

[15] Heon M, Lofland S, Applegate J, Nolte R, Cortes E, Hettinger JD, et al. Continuous carbide-derived carbon films with high volumetric capacitance. Energy Environ Sci 2011;4:135–8.

[16] Liu F, Gutes A, Laboriante I, Carraro C, Maboudian R. Graphitization of n-type polycrystalline silicon carbide for on-chip supercapacitor application. Appl Phys Lett 2011;99:112104.

[17] El-Kady MF, Kaner RB. Scalable fabrication of high-power graphene micro-supercapacitors for flexible and on-chip energy storage. Nat Commun 2013;4:1475.

[18] Niu Z, Zhang L, Liu L, Zhu B, Dong H, Chen X. All-solid-state flexible ultrathin micro-supercapacitors based on graphene. Adv Mater 2013;25:4035–510.

[19] Le LT, Ervin MH, Qui H, Fuchs BE, Zunio J, Lee WY. Inkjet-printed graphene for flexible micro-supercapacitors. Proc IEEE-NANO 2011:67–71.

[20] Huang Y, Liang J, Chen Y. An overview of the applications of graphene-based materials in supercapacitors. Small 2012;8:1805–34.

[21] Beidaghi M, Wang C. Micro-supercapacitors based on interdigital electrodes of reduced graphene oxide and carbon nanotube composites with ultra high power handling performance. Adv Funct Mater 2012;22:4501–10.

[22] Lin J, Zhang C, Yan Z, Zhu Y, Peng Z, Hauge RH, et al. 3-Dimensional graphene carbon nanotube carpet-based microsupercapacitors with high electrochemical performance. Nano Lett 2013;13:72–8.

[23] Hsia B, Kim MS, Vincent M, Carraro C, Maboudian R. Photoresist-derived porous carbon for on-chip micro-supercapacitors. Carbon 2013;57:395–400.

[24] Wang K, Zou W, Quan B, Yu A, Wu H, Jiang P, et al. An all-solid-state flexible micro-supercapacitor on a chip. Adv Energy Mater 2011;1:1068–72.

[25] Tseng SH, Tai NH. Fabrication of a transparent and flexible thin film transistor based on single-walled carbon nanotubes using the direct transfer method. Appl Phys Lett 2009;95:204104.

[26] Tsai TY, Lee CY, Tai NH, Tuan WH. Transfer of patterned vertically aligned carbon nanotubes onto plastic substrates for flexible electronics and field emission devices. Appl Phys Lett 2009;95:013107.

[27] Jenkins GM, Kawamura K. Polymeric carbons – carbon fiber, glass and char. London: Cambridge University Press; 1976.

[28] Ranganathan S, McCreery RL. Electroanalytical performance of carbon films with near-atomic flatness. Anal Chem 2001;73:893–900.

[29] Niu J, Pell WG, Conway BE. Requirements for performance characterization of C double-layer supercapacitors: applications to a high specific-area C-cloth material. J Power Sources 2006;40:156–725.

[30] Chen WC, Wen TC. Electrochemical and capacitive properties of polyaniline implanted porous carbon electrode for supercapacitors. J Power Sources 2003;117:273–82.

[31] Gogotsi Y, Simon P. True performance metrics in electrochemical energy storage. Science 2011;334:917–8.

[32] Miller JR. Valuing reversible energy storage. Science 2012;335:1312–3.

[33] Stoller MD, Ruoff RS. Best practice methods for determining an electrode material's performance for ultracapacitors. Energy Environ Sci 2010;3:1294–301.

[34] Song HK, Hwang HY, Lee KH, Dao LH. The effect of pore size distribution on the frequency dispersion of porous electrodes. Electrochim Acta 2000;45:2241–57.